PAA-3001、コントロール装置 PA-2010A;小原医科産業株式会社、図 6）を用い、嫌悪刺激の 24 時間後における学習成績について検討した。なお、1 回目の嫌悪刺激は 0.3 mA 電流を 5 秒間であり、2 回目は 0.3 mA 電流を 3 秒間であった。

＜新奇物体認知試験＞OVX した 12～13 週齢 WI 雌ラット：黒色塩化ビニル製ケージを用い、弁別法による物体に対する探索行動を指標として、学習成績について検討した。なお 1 回目の実験で、物体の選好性に化学物質曝露の影響が検出されたため、物体を変更して 2 回目を行った。

＜社会性認知試験＞OVX した 16 週齢 WI 雌ラット：ステンレス製格子等で 3 部屋に区切られた黒色塩化ビニル製 3 チャンバーケージに予めテストラットを慣らし、未知の相手雌ラットを 1 匹入れ探索行動をさせ社会性の強度を検討した（獲得試行：図 7）。その後チャンバーから 2 匹を取出し、インターバルの後テストラットおよびさきほどの未知ラットを既知ラットとして、さらに別の未知雌ラットを新たな未知ラットとして入れ、既知・未知ラット各々へのテストラットの接近回数・接近時間を測定し、社会性認知を検討した（保持試行）。相手雌ラットは OVX した 15 週齢の WI ラットを用いた。

＜母子分離誘発啼鳴反応＞0 週齢 WI 雌ラット：生後 24 時間以内に oil あるいは E2 を曝露した動物を用い、母親および同腹仔から引き離されると発する、20 kHz～60 kHz の超音波領域に主成分を持つ啼鳴反応を測定した。また、生後 24 時間以内に何も曝露していない動物を用い、啼鳴反応における 30 分前のジアゼパム 0.03 mg/kg 投与の影響が、性差を有するか否か検討した。

（倫理面への配慮）

動物実験は明治大学農学部動物実験委員会委員の許可の下で行った。行動実験はラットに対し堪え難い程の苦痛を与えないレベルで行った。

C．研究結果

＜性選好性試験＞生後 24 時間以内の EE 及び陽性対照である E2 曝露は性選好性を消失させた。また、EE 曝露による性選好性への影響は濃度依存的に表れた（表 1）。

＜性行動試験＞生後 24 時間以内の 2 mg/kg EE 曝露は陽性対照である E2 よりは弱かったが、成熟後の WI 雌ラットの性行動を抑制した（図 8）。

＜エストロゲン受容体 α 発現量測定＞視索前野では、実験 48 時間前 EB 投与をしなかった場合に、生後 24 時間以内の 20 μg/kg EE 曝露でエストロゲン受容体 α 発現量が増加した。しかし、実験 48 時間前 EB 投与をした場合は、生後 24 時間以内 EE 曝露の影響は消失した。視床下部内側基底部では、実験 48 時間前 EB 投与をしなかった場合の群間の差は検出されなかったが、実験 48 時間前 EB 投与をした場合は生後 24 時間以内の 20 μg/kg EE 曝露でエストロゲン受容体 α 発現量が増加した。

＜オープンフィールド試験＞無処置 5 週齢及び、OVX11 週齢 WI 雌ラットにおいて、活動量の指標である総移動距離・平均移動速度にはエストロゲン様物質投与は影響を及ぼさなかった。また、実験 24 時間前 EB 投与の有無による影響も検出されなかった。

＜高架十字試験＞OVX12 週齢 WI 雌ラットの oil 群において、実験 24 時間前 EB 投与により不安様行動の減弱が見られたが、曝露群では EB 投与の影響は消失した。

＜受動回避学習試験＞2 回実験を繰り返し、1 回目では実験 24 時間前 EB 投与の場合に、生後 24 時間以内の 20 μg/kg EE 曝露で学習の低下が認められたが、2 回目では認められなかった。

＜新奇物体認知試験＞OVX した 12～13 週齢 WI 雌ラットにおいて、1 回目では生後 24 時間以内の 20 μg/kg EE 曝露で物体認知が低下した。しかし、物体を変更して行った 2 回目においては、その影響を検出することができなかった。

＜社会性認知試験＞未知ラットへの接近

行動には群間に有意差は認められなかったが、その後の既知ラットと未知ラットの同時提示では、oil と E2 曝露においてのみ未知ラットへの接近が既知ラットに比べ有意に増加した。

＜母子分離誘発啼鳴反応＞0 週齢 WI 雌ラットにおいて、母子分離後の啼鳴反応には生後 24 時間以内の E2 曝露の影響はみられなかった（表 2）。また、母子分離誘発啼鳴反応 30 分前のジアゼパム 0.03 mg/kg 投与は、母子分離誘発啼鳴反応を減弱させるが、その影響に性差は検出されなかった。

D．考察

本年度改めて性選好性試験において検定を追加した結果、前・本年度に行った両実験において、陽性対照の E2 曝露や 2 mg/kg EE 曝露のみならず、20 μg/kg EE 曝露でも性選好性が消失した。総合的に考えると、生後 24 時間以内の EDs 曝露は濃度依存的に性選好性を抑制するものと考えられえる。一方性行動は、前回同様 2 mg/kg EE 曝露及び E2 曝露で低下が見られたが、本年度は E2 曝露でより強く影響が表れた。このことは、画像解析の解像度を上げ、より解析精度が正確になったことも影響している可能性があり、本年度の結果の方が信憑性は高いと考えられる。

エストロゲン受容体 α 発現量は、今回の結果では 20 μg/kg EE 曝露においてのみ、視索前野では実験 48 時間前 EB 投与をしなかった場合に、視床下部内側基底部では実験 48 時間前 EB 投与をした場合に増加した。この変化は、性行動及び性選好性の結果と一致しない。従って、エストロゲン受容体 α 発現への生後 24 時間以内の EDs 曝露の影響は脳領域により異なり、さらにエストロゲン感受性も部位特異的に変化させる可能性が示された。

オープンフィールド試験の総移動距離、平均移動速度においては、前回と同様、本実験による化学物質曝露による影響は検出されなかった。また本年度は OVX のみならず、OVX に加えて EB 急性曝露がオープンフィールド試験に影響する可能性を検討したが、有意な影響は検出されなかった。従って、活動量においては本研究で用いた EDs 曝露は影響しないことが示された。

高架十字試験においては、実験 24 時間前の EB 投与により oil 群の不安様行動の減弱が見られたが、EE・E2 曝露群では EB 投与の影響は消失したことから、エストロゲン感受性が変化した可能性がある。一方、前年度では 20 μg/kg EE 曝露で不安様行動の減弱が認められたが、今回は検出されなかった。これは、前年度において受動回避試験を先に行っていることが影響している可能性があり、今後検討を要するが、本試験で用いた EE・E2 曝露の不安への影響はあるとしても軽微である可能性が高い。

受動回避試験に用いた動物は、学習行動へのエストロゲン感受性を明らかにするために、本年度は OVX し半分は実験 24 時間前に EB 投与した結果、EB 投与条件下で 20 μg/kg EE 曝露群における学習能力が低下傾向を示した。これは前年度の無処置動物での結果と類似しており、20 μg/kg EE 曝露で学習行動が低下した原因の一部は脳におけるエストロゲン感受性に起因している可能性を示している。しかし、実験を繰り返したが同じ結果が得られなかった。これは実験条件の違いが影響を及ぼしている可能性が高いが、今後検討を要する。

新奇物体認知試験 1 回目において 20 μg/kg EE 曝露での物体認知の低下が検出されたが、2 回目では検出することができなかった。これは、物体を変更したことが結果の不一致に影響している可能性がある。今後さらに方法を改善し、検討する必要がある。

社会性認知試験では、未知ラット単体提示における接近行動には群間に有意差は検出されなかったため、社会性行動そのものには本実験の曝露は影響していない可能性が高い。また、未知・既知ラット同時提示

における未知ラットに対する接近が既知ラットに比べて有意に多かった oil 群と E2 曝露群では、同種の個体識別、つまり社会性認知能力があることが示された。一方、20 μg/kg EE 曝露と 2 mg/kg EE 曝露では有意な影響が認められなかったことから、社会性認知能力が低下している可能性が示唆された。従って本研究の EE 曝露は、E2 とは異なる独自の機序により社会性認知能力を低下させる、あるいは陽性対照より低濃度の EDs が社会性認知能力を低下させる可能性がある。

早期指標の確立を目指して、母子分離誘発啼鳴反応の生後 24 時間以内 E2 曝露の影響を検討したが、曝露による影響は検出されなかった。また、成熟動物の一部の行動において抑制影響に性差が見られるジアゼパムを投与することにより、母子分離誘発啼鳴反応の性差を検出できるのではないかと考え検討したが、明らかな影響は検出されなかった。従って、早期指標としては他の項目を検討する必要がある。

E．結論

2 mg/kg といった高い濃度の EE 臨界期曝露は雌ラットの性選好性および性行動を低下させた。また性選好性においては 20 mg/kg EE 曝露においてもある程度の減弱を示したため、性選好性のエストロゲン様物質曝露に対する感受性は性行動より高い可能性が示された。エストロゲン受容体 α 発現量は、部位特異的な発現変化が示された。不安・学習行動への生後 24 時間以内の EDs 曝露は影響は軽微なものの、成熟後のエストロゲン感受性を変化させる可能性が示された。一方、活動量へはエストロゲン感受性も含め、いずれの曝露も影響を及ぼさないことを明らかとした。

F．研究発表

1. 論文発表

1）Y. Horii, M. Kawaguchi (corresponding), R. Ohta, A. Hirano, G. Watanabe, N. Kato, T. Himi, and K. Taya.
Male hatano high-avoidance rats show high avoidance and high anxiety-like behaviors as compared with male low-avoidance rats.
Exp. Anim., 2012 Sep;61(5): 517–524

2. 学会発表

1）千本隆志、小林由紀、近藤保彦、川口真以子
出生直後のethynyl estradiol曝露がラットの学習行動に及ぼす影響
第17回日本行動内分泌研究会（2012年8月31日、京都）

2）小峰千亜希、近藤保彦、植村英恵、千本隆志、川口真以子
出生直後の雌ラットethynyl estradiol曝露が成熟後の性行動に及ぼす影響
第105回日本繁殖生物学会大会（2012年9月6-7日、茨城）

3）小田島夢花、宮田能、中島春香、近藤保彦、吉田緑、川口真以子
生後24時間以内の雌ラットへのethynyl estradiol曝露が成熟後の性選好性に与える影響
第15回環境ホルモン学会研究発表会（2012年12月18-19日、東京）

4）朝川比登美、千本隆志、神島愛美、小林由紀、吉田緑、川口真以子
生後24時間以内の雌ラットへのethynyl estradiol曝露が成熟後の探索行動に与える影響
第15回環境ホルモン学会研究発表会（2012年12月18-19日、東京）

5）志賀健臣、溝口康、川口真以子
生後24時間以内の雌ラットへのEthynyl estradiol曝露が成熟後のエストロゲン受容体α発現に及ぼす影響
第15回環境ホルモン学会研究発表会（2012年12月18-19日、東京）

6）Kamishima M, Kobayashi Y, Senbon T, Komine C, Uemura H, Yoshida M, Kondo Y, Kawaguchi M
EFFECTS OF NEONATAL SINGLE

INJECTION OF ETHINYL ESTRADIOL ON FEEDING, LEARNING AND SEXUAL BEHAVIORS IN ADULT FEMALE RATS. The 17th FAVA Congress（2013年1月5-6日、Taipei、Taiwan）

G．知的財産権の出願・登録状況

10. 特許取得
    該当なし
11. 実用新案登録
    該当なし
12. その他
    該当なし

参考文献

(1) Sexually dimorphic expression of hypothalamic estrogen receptors α and β and kiss1 in neonatal male and female rats. Cao J, Patisaul HB, *J. Comp. Neurol.*, 2011, Epub ahead of print.

(2) Cellular mechanisms of estradiol-mediated sexual differentiation of the brain., Wright CL, Schwarz JS, Dean SL, et. al., *Trends Endocrinol Metab*, 2010, 21, 553-61.

(3) Bisphenol A: developmental toxicity from early prenatal exposure. Golub MS, Wu KL, Kaufman FL, et. al., *Birth Defects Res B Dev Reprod Toxicol.* 2010, 89, 441-66.

(4) Sexual differentiation of the rodent hypothalamus: hormonal and environmental influences., Negri-Cesi P, Colciago A, Pravettoni A, et.al., *J Steroid Biochem Mol Biol.*, 2008, 109, 294-9.

(5) Effects of developmental exposure to bisphenol A on brain and behavior in mice., Palanza P, Gioiosa L, vom Saal FS, et. al., *Environ Res.* 2008, 108, 150-7.

(6) Female sexual maturation and reproduction after prepubertal exposure to estrogens and endocrine disrupting chemicals: a review of rodent and human data., Rasier G, Toppari J, Parent AS, et. al., *Mol Cell Endocrinol.* 2006, 254-255, 187-201.

(7) Estrogen Receptor Gene Promoter 0/B Usage in the
Rat Sexually Dimorphic Nucleus of the Preoptic Area., Hamada T and Sakuma Y, *Endocrinology*, 2010, 151(4), 1923-1928.


図1 Estrogen（E2）が引き起こす作用
形成作用
不可逆的
出生前後の一時期
活性作用
可逆的
主に成熟後
中枢神経系の
形態・回路が
固定化される
中枢神経系の
活動が
賦活される


図2 E2が作用する中枢神経系の機能
情動
摂食
高次機能
学習・記憶
生殖
E2
卵巣

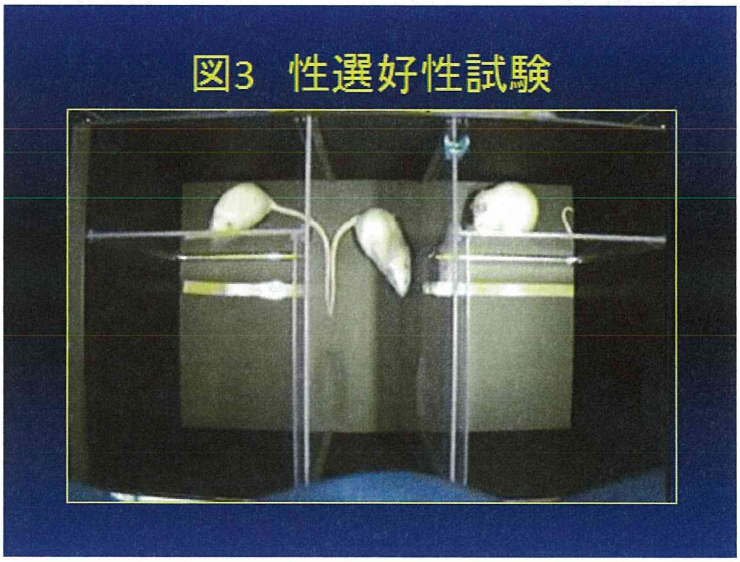
図3 性選好性試験

図4　円形オープンフィールド

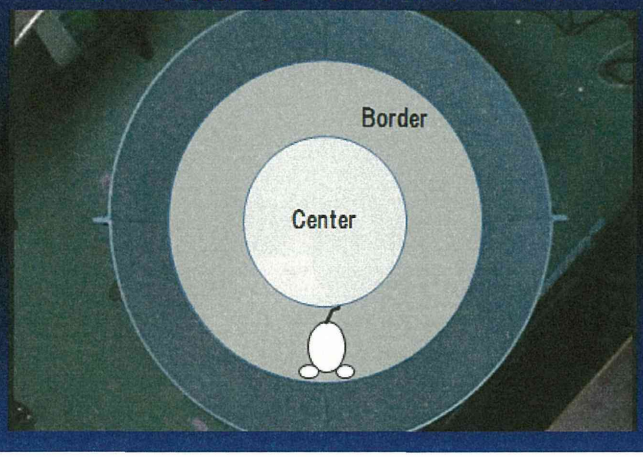

図5　高架十字

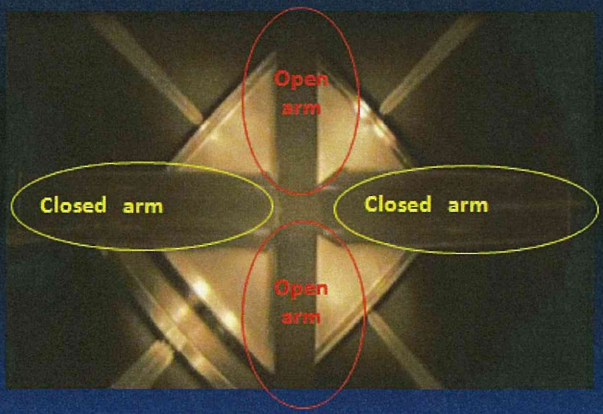

図6　受動回避学習試験装置

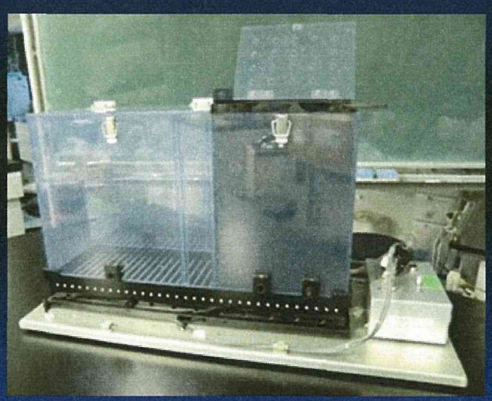

図7　社会性認知試験

個別飼育10日間 ハンドリング、フィールドへの馴化3日間

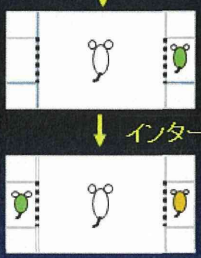

訓練試行
（社会性行動測定）

インターバル

保持試行
（社会性認知測定）

行動を録画し、画像解析ソフトEthovision XT8で動物の鼻が相手ケージへ接触する回数と時間を解析する

表1　10～14週齢WI雌ラットの性選好性試験結果

接近回数

	実験①	実験②
1回目 雄への接近回数	high EE↓	―
性選好性の有無	high EE×、E2×	E2×
2回目 雄への接近回数	―	E2↓
性選好性の有無	high EE×、E2×	high EE×、E2×

接近時間

	実験①	実験②
1回目 雄への接近時間	E2↓	E2↓
性選好性の有無	E2×	E2×
2回目 雄への接近時間	―	E2↓
性選好性の有無	low EE×、high EE×、E2×	low EE×、high EE×、E2×

図8　13～14週齢WI雌ラットの性行動試験結果

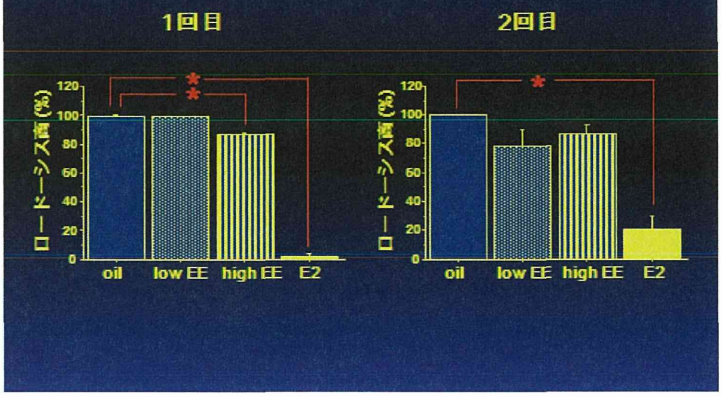

Ⅲ. 研究成果の刊行に関する一覧表

雑誌

著者名	タイトル	雑誌名	管・号・ページ	年
Taketa Y, Yoshida M, Inoue K, Takahashi M, Sakamoto Y, Watanabe G, Taya K, Yamate J, Nishikawa A.	The newly formed corpora lutea of normal cycling rats exhibit drastic changes in steroidogenic and luteolytic gene expressions.	Exp Toxicol Pathol.	64(7-8):775-82.	2012
Takahashi M, Matsuo S, Inoue K, Tamura K, Irie K, Kodama Y, Yoshida M.	Development of an early induction model of medulloblastoma in Ptch1 heterozygous mice initiated with N-ethyl-N-nitrosourea	Cancer Sci.	103(12):2051-5	2012
Yoshida M, Katsuda S, Maekawa A.	Involvements of Estrogen Receptor, Proliferating Cell Nuclear Antigen and p53 in Endometrial Adenocarcinoma Development in Donryu Rats.	J Toxicol Pathol.	25(4):241-7	2012
Taketa Y, Inoue K, Takahashi M, Yamate J, Yoshida M.	Differential Morphological Effects in Rat Corpora Lutea among Ethylene Glycol	Toxicol Pathol.	In press	2012
Y. Horii, M. Kawaguchi (corresponding), R. Ohta, A. Hirano, G. Watanabe, N. Kato, T. Himi,	Male hatano high-avoidance rats show high avoidance and high anxiety-like behaviors as compared with male low-avoidance rats.	Exp. Anim	Sep;61(5): 517–524	2012

and K. Taya.				
Shirota M, Kawashima J, Ogawa Y, Kamiie J, Yasuno K, Shirota K, Yoshida M.	Delayed effects of single neonatal subcutaneous exposure of low-dose 17α-ethynyl estradiol on reproductive function in female rats.	Journal of Toxicological Sciences	37: 681-689	2012
Shirota M, Kawashima J, Nakamura T, Ogawa Y, Kamine J, Shirota K.	Vascular Hamartoma in the Uterus of a Female Sprague-Dawley Rat with an Episode of Vaginal	Toxicol Pathol	In press	2013
Matsuo S, Takahashi M, Inoue K, Tamura K, Irie K, Kodama Y, Nishikawa A, Yoshida M.	Thickened area of external granular layer and Ki-67 positive focus are early events of medulloblastoma in Ptch1(+/-) mice.	Exp Toxicol Pathol.	In press	2013

. ,

Ⅳ. 研究成果の刊行物

Experimental and Toxicologic Pathology 64 (2012) 775–782

Contents lists available at ScienceDirect

Experimental and Toxicologic Pathology

journal homepage: www.elsevier.de/etp

The newly formed corpora lutea of normal cycling rats exhibit drastic changes in steroidogenic and luteolytic gene expressions

Yoshikazu Taketa[a,b], Midori Yoshida[a,*], Kaoru Inoue[a], Miwa Takahashi[a], Yohei Sakamoto[a], Gen Watanabe[c], Kazuyoshi Taya[c], Jyoji Yamate[b], Akiyoshi Nishikawa[a]

[a] Division of Pathology, National Institute of Health Sciences, 1-18-1 Kamiyoga, Setagaya-ku, Tokyo 158-8501, Japan
[b] Laboratory of Veterinary Pathology, Life and Environmental Sciences, Osaka Prefecture University, 1-58 Rinkuu Ourai Kita, Izumisano, Osaka 598-8531, Japan
[c] Laboratory of Veterinary Physiology, Department of Veterinary Medicine, Faculty of Agriculture, Tokyo University of Agriculture and Technology, 3-5-8 Saiwai-cho, Fuchu, Tokyo 183-8509, Japan

ARTICLE INFO

Article history:
Received 27 July 2010
Accepted 30 January 2011

Keywords:
Corpora lutea
Estrous cycle
Laser microdissection
Progesterone
Rat

ABSTRACT

In normal estrous cycling rats, corpora lutea (CL) regress over several cycles; however, the period during which they secrete progesterone (P4) is strictly limited. In the present study, we clarified the function of CL in normal cycling rats. We especially focused on expression levels of four steroidogenic and two luteolytic genes in the two different populations of the CL (new and old CL) at each estrous stage. The ovaries of female rats at each estrous cycle were collected, and new and old CL were separated with laser microdissection and analyzed for mRNA expression. In the new CL, the expressions of scavenger receptor class B type I (*SR-BI*), steroidogenic acute regulatory protein (*StAR*), and P450 cholesterol side-chain cleavage (*P450scc*) mRNA reached their highest levels at metestrus, and 3β-hydroxysteroid dehydrogenase (3β-*HSD*) mRNA gradually increased from estrus to diestrus. Meanwhile, 20α-hydroxysteroid dehydrogenase (20α-*HSD*) and prostaglandin F2 alpha receptor (*PGF2α-R*) mRNA levels were remarkably low from estrus to metestrus and gradually increased thereafter. These gene levels in new CL corresponded to serum P4 levels during the estrous cycle. In the old CL, all steroidogenic and luteolytic gene levels were consistently high throughout the estrous cycle. These results provide clear evidence that new CL at metestrus have strong steroidogenic activity and through inhibition of luteolysis, maintain P4 production in normal cycling rats. The elevation of 20α-HSD and PGF2α-R levels in new CL at diestrus may be a trigger of functional luteolysis.

1. Introduction

Numerous drugs and chemicals that have been tested in experimental animals have been found to interfere with reproductive function in the female (Yuan and Foley, 2002). These chemicals, which usually target the ovaries, are commonly referred to as ovarian toxicants and frequently cause disturbances in estrous cyclicity in rodents. Other chemicals may act by altering the normal morphology of the reproductive tract (Yoshida et al., 2009). For instance, 4-vinyl-cyclohexene diepoxide (VCD) destroys oocytes and induces the decrease of small follicles (Ito et al., 2009), and ethylene glycol monomethyl ether (EGME) stimulates luteal progesterone (P4) secretion and induces luteal hypertrophy (Dodo et al., 2009). The ovary has two distinct functional components required for estrous cyclicity, the corpora lutea (CL) and the follicles. Understanding the morphology and function of these structures is a prerequisite for understanding the mechanism of ovarian toxicants that disrupt the estrous cycle. The rat estrous cycle is characterized by cyclic variation in P4 levels. There are two discrete periods in the estrous cycle during which P4 is increased. The first occurs in the afternoon of proestrus and the second during the metestrus to diestrus stages (Smith et al., 1975; Tebar et al., 1995). The preovulatory P4 is secreted during proestrus by the Graafian follicles in an luteinizing hormone (LH)-dependent manner. In metestrus and diestrus, secretion is from the CL in an LH-independent manner. The luteal secretion of P4 during the metestrus to diestrus stages begins to rise in the morning of metestrus, reaches peak values by midnight of metestrus, and falls to basal levels thereafter as a result of luteolysis (Kaneko et al., 1986). This drop-off in P4 is considered the beginning of the functional regression of the CL in the normal rat estrous cycle. Additionally, prolactin (PRL) has a crucial role in luteal P4 secretion and structural luteolysis (Stocco et al., 2007).

The P4 biosynthesis in the CL is divided into the following two steps: the uptake, synthesis, and transport of cholesterol, and the processing of cholesterol to P4. Cholesterol is preferentially yielded from circulatory high- and low-density lipoproteins (HDL and LDL);

* Corresponding author. Tel.: +81 3 3700 9821; fax: +81 3 3700 1425.
E-mail address: midoriy@nihs.go.jp (M. Yoshida).

0940-2993/$ – see front matter © 2011 Elsevier GmbH. All rights reserved.
doi:10.1016/j.etp.2011.01.015

and HDL is the main source of cholesterol for CL in rodents (Bruot et al., 1982; Schuler et al., 1981). Scavenger receptor class B type I (SR-BI) is now considered as the authentic HDL receptor mediating the selective uptake of HDL-derived cholesterol ester (Acton et al., 1996). After uptake, the cholesterol esters are transported to the outer mitochondrial membrane and then to the inner membrane by several proteins including steroidogenic acute regulatory protein (StAR) (Stocco et al., 2001). Once cholesterol reaches the inner mitochondrial membrane, its transformation into P4 begins. In this step, mitochondrial P450 cholesterol side-chain cleavage (P450scc) (Oonk et al., 1989) and 3β-hydroxysteroid dehydrogenase (3β-HSD) which are located in the smooth endoplasmic reticulum (Peng et al., 2002) play principal roles.

The P4 secretion from the CL in rodents is regulated by the balance between synthesis and catabolism. Briefly, it depends not only on the amount of P4 synthesized by the luteal cells but also on the expression of the enzyme 20α-hydroxysteroid dehydrogenase (20α-HSD) that catabolizes P4 into the inactive progestin, 20α-dihydroprogesterone (20α-DHP). Once 20α-HSD becomes expressed in the CL, P4 secretion declines and 20α-DHP becomes the major steroid secreted by luteal cells (Stocco et al., 2000).

In rodents, the decrease in P4 is an index of the functional regression of the CL. The structural regression occurs after the initial decline in P4 output and is morphologically observed as luteal cell apoptosis (Stocco et al., 2007). In the functional regression, several factors including prostaglandin F2 alpha (PGF2α) and LH have been implicated in the downregulation of luteal P4 production (Pharriss and Wyngarden, 1969; Plas-Roser et al., 1988). Meanwhile, several signals including PRL, PGF2α, tumor necrosis factor-alpha (TNFα), and Fas ligand (FasL) have been indicated in the induction of cell death required for the structural regression of the CL (Gaytan et al., 2000; Roughton et al., 1999; Stocco et al., 2007; Yadav et al., 2005).

There are two main types of CL: those which are newly formed by the current ovulation (new CL) and CL remaining from prior estrous cycles (old CL) (Bowen and Keyes, 2000). New and old CL are morphologically distinguishable at each estrous stage, and new CL drastically change their morphology during the estrous cycle (Yoshida et al., 2009).

As mentioned above, the CL in cycling rats secrete P4 for a limited period prior to undergoing functional luteolysis a few days after being formed. It is likely that both new and old CL are essential to estrous cycle regulation. Therefore, it is important to analyze normal functional changes of steroidogenesis in each type of CL across the estrous cycle in order to understand how they may be affected by ovarian toxicants. The expression of steroidogenic and luteolytic factors across the estrous cycle has been partially elucidated (Peluffo et al., 2006; Slot et al., 2006; Takahashi et al., 1995); however, little is known about the transitions in gene expression that occur in new and old CL across the estrous cycle. In the present study, we investigated the transitions in luteal gene expression and steroidogenesis in each rat estrous stage to identify the potential targets of ovarian toxicants. We separated new CL from old CL using laser microdissection (LMD). We focused on four steroidogenic genes: *SR-BI*, *StAR*, *P450scc*, and 3β-*HSD*, and two luteolytic genes: 20α-*HSD* and PGF2α receptor (*PGF2α-R*). Additionally, immunohistochemical features of P450scc and 3β-HSD in both types of CL were also examined.

2. Materials and methods

2.1. Animals

Female 6-week-old Sprague–Dawley (Crl:CD) rats were purchased from Charles River Laboratories Japan, Inc. (Yokohama, Japan). They were housed in plastic cages (3 or 4 animals/cage) maintained at 23–25 °C and a relative humidity of 50–60% with a 12-h light cycle. Commercial rodent chow (CRF-1; Oriental Yeast Co., Ltd., Tokyo, Japan) and drinking water were available *ad libitum* throughout the experiment. The animal protocols were reviewed and approved by the Animal Care and Use Committee of the National Institute of Health Sciences, Japan.

Estrous cyclicity was monitored by daily vaginal smears. When the rats reached 10 weeks of age, they were euthanized by decapitation at each of the estrous stages (estrus, metestrus, diestrus, and proestrus: 6–7 rats per group) between 10:00 and 12:00 AM. These estrous stages were also confirmed by microscopic examination of the vagina and uterus. For LMD, the left ovaries were rapidly removed, embedded in OCT compound, and frozen with liquid nitrogen. The right ovaries were fixed in 4% paraformaldehyde for one day, and routinely processed with hematoxylin and eosin (HE) and immunohistochemical stains.

2.2. Laser microdissection of new or old corpora lutea in each estrous stage

The OCT-embedded frozen ovaries were sectioned into 10 μm slices onto membrane-based laser microdissection slides (Leica Microsystems, Wetzlar, Germany) and fixed in 70% ethanol for 1 min. The sections were then hydrated in diethylpyrocarbonate (DEPC)-treated water for 10 s, stained with toluidine blue for 30 s, washed in DEPC water for 30 s, dehydrated by dipping sequentially in 70, 95, and 100% ethanol and then air dried. New CL (CL which are newly formed by the current ovulation) and old CL (CL remaining from prior estrous cycles) were visualized and captured using a Leica LMD6000 laser microdissection system (Leica Microsystems) (Sakurada et al., 2006).

2.3. Extraction of total RNA and reverse transcription

Laser-captured tissues were pooled in lysis buffer and RNA was extracted with the RNeasy Mini kit (Qiagen, Valencia, CA, USA) according to the manufacturer's instructions. Residual genomic DNA was removed by an on-column RNase-free DNase Set (Qiagen) during RNA purification. The RNA was then precipitated with 14 μl ddH_2O, checked for concentration and purity using the spectrophotometer (NanoDrop ND-1000, Thermo Fischer Scientific Inc., Waltham, MA, USA), and stored at −80 °C until analysis. For cDNA synthesis, reverse transcription (RT) was performed with the Sensiscript RT Kit (Qiagen) using random primers in a 20 μl final volume following the manufacturer's instructions.

2.4. Real-time quantitative PCR

Messenger RNA levels were analyzed using an ABI Prism 7900 Sequence Detection System and TaqMan® gene expression assays (Applied Biosystems, Foster City, CA, USA) for *SR-BI*, *StAR*, *P450scc*, 3β-*HSD*, 20α-*HSD*, *PGF2α-R*, and hypoxanthine-guanine phosphoribosyltransferase (*HPRT*) (Table 1). The PCR cycling conditions included an initial denaturation at 95 °C for 20 s followed by 50 cycles at 95 °C for 1 s and 60 °C for 20 s. To compare mRNA levels among samples, mRNA for each gene of interest was normalized to the expression of a housekeeping gene, *HPRT*, using the standard curve method. Real-time PCR reactions were performed with the Universal TaqMan 2× Fast Universal PCR Master Mix (Applied Biosystems) in a 20 μl reaction volume.

2.5. Immunohistochemistry

The right ovarian sections were deparaffinized, treated with 90% methanol containing 3% H_2O_2 for 10 min at room tempera-

Table 1
Primers and probes used for real-time PCR analysis.

Gene	Primer and probe		GenBank accession No.
SR-BI	Forward	5′-CCGAATCCTCACTGGAATTCTTC-3′	NM_031541
	Reverse	5′-CGAACACCCTTGATTCCTGGTA-3′	
	Probe	5′-VIC-AAGCCTGCAGATCTATGA-MGB-3′	
StAR	Forward	5′-GGGAGAGTGGAACCCAAATGT-3′	NM_031558
	Reverse	5′-CATGGGTGATGACTGTGTCTTTTC-3′	
	Probe	5′-VIC-AAGGAAATCAAGGTCCTGAAG-MGB-3′	
P450scc	Forward	5′-TCTCCTCTACCAACAGTCCTCGAT-3′	BC089100
	Reverse	5′-TGGTACAGGTTTATCCAACCATTG-3′	
	Probe	5′-VIC-CTTCAATGAGATCCCTTC-MGB-3′	
3β-*HSD*	Forward	5′-GCCCAACTCCTACAAGAAGATCAT-3′	L17138
	Reverse	5′-CTCGGCCATCTTTTTGCTGTATG-3′	
	Probe	5′-VIC-ATGTGCTTTCATGATGCTCT-MGB-3′	
20α-*HSD*	Forward	5′-TTTCAATGAGGAGAGAATCAGAGAGA-3′	L32601
	Reverse	5′-CCATGTCATCTGAAGCCAACTG-3′	
	Probe	5′-VIC-CCTGCAGGTCTTTGAT-MGB-3′	
PGF2α-R	Forward	5′-CTCTGGCTTGTGCCCACTTT-3′	U47287
	Reverse	5′-CCGATGCACCTCTCAATGG-3′	
	Probe	5′-VIC-CCTGGGCAGTACGATG-MGB-3′	
HPRT	Forward	5′-GCCGACCGGTTCTGTCAT-3′	X62085
	Reverse	5′-GGTCATAACCTGGTTCATCATCAC-3′	
	Probe	5′-FAM-CAGTCCCAGCGTCGTG-TAMRA-3′	

ture (RT), and washed twice in PBS. For P450scc immunostaining, sections were heated in a citric acid buffer 0.01 M (pH = 7.0) at 95 °C for 5 min and washed twice in PBS. For 3β-HSD immunostaining, there was no antigen retrieval treatment. A blocking solution was then applied for 30 min. The blocking solutions were 3% goat serum in PBS for P450scc and 3% rabbit serum in PBS for 3β-HSD. Sections were then incubated overnight with P450scc antibody (1:200; Millipore Corporation, Temecula, CA, USA) or 3β-HSD antibody (1:200; Santa Cruz, CA, USA) at 4 °C. After washing 4 times in PBS, the sections were then incubated with the secondary antibody (HISTOFINE SIMPLESTAIN MAX-PO, Nichirei Bioscience, Tokyo, Japan) matched to the primary antibody for 30 min at RT. The reaction products were visualized with 3,3′-diaminobenzidine (DAB, Dojindo Laboratories, Kumamoto, Japan). The sections were counterstained with Mayer's hematoxylin. To test the specificity of immunostaining, negative controls were run without the primary antibodies.

2.6. Hormone assays

Serum samples obtained after decapitation were stored at −80 °C until assay. The serum concentrations of follicle-stimulating hormone (FSH), LH, inhibin-α (INH), PRL, estradiol-17β (E_2), and P4 were determined using double-antibody radioimmunoassay and ^{125}I-labeled radioligands. National Institute of Diabetes and Digestive and Kidney Disease (NIDDK) radioimmunoassay kits were employed for rat FSH, LH, and PRL (NIAMDD, NIH, Bethesda, MD, USA) as described by Taya et al. (1983). Immunoreactive INH in the serum was analyzed using a rabbit anti-serum, TNDH-1 (Hamada et al., 1989). The serum concentrations of E_2 and P4 were also measured as described by Taya et al. (1985).

2.7. Statistical analysis

Hormonal data are presented as the mean ± SEM. Real-time PCR data are presented as the mean ± SD. Variances in data of hormone concentrations and relative mRNA levels of new and old CL across the estrous cycle were checked for homogeneity by Bartlett's procedure. If the variance was homogeneous, the data were assessed by one-way ANOVA. If not, the Kruskal–Wallis test was applied. When statistically significant differences were indicated, the Dunnett's multiple test was employed. Differences of mRNA level between new and old CL for each estrous stage were evaluated by Welch's *t*-test. $P < 0.05$ was considered statistically significant.

3. Results

3.1. Changes of serum hormone levels during the estrous cycle

The serum P4 and LH levels were significantly higher at metestrus, and the E_2 level was gradually elevated from estrus to proestrus (Fig. 1). The concentrations of PRL, FSH, and INH were not significantly different across the estrous cycle (Fig. 1).

3.2. Expressions of steroidogenic and luteolytic genes in new and old CL during the estrous cycle

The changes in mRNA expression for each estrous stage in new and old CL are shown in Figs. 2 and 3. In the new CL, the levels of *SR-BI*, *StAR* and *P450scc* mRNA reached their highest values at metestrus and gradually decreased thereafter (*SR-BI*; 544, 228, and 113%, *StAR*; 596, 407, and 325%, *P450scc*; 231, 146, and 68% at metestrus, diestrus, and proestrus, respectively, compared to estrus) (Fig. 2A–C). There were no differences in the levels of these genes in old CL throughout the estrous cycle (Fig. 2A–C). The expression of 3β-*HSD* mRNA was gradually increased from estrus to diestrus in new CL, but decreased at proestrus (155, 172, and 121% at metestrus, diestrus, and proestrus, respectively, compared to estrus) (Fig. 2D). 3β-*HSD* mRNA expression in old CL showed a similar change, though to a consistently lesser degree (Fig. 2D). In the new CL, 20α-*HSD* and *PGF2α-R* mRNA levels were extremely low at estrus and metestrus, and drastically increased from diestrus to proestrus (20α-*HSD*; 92, 4587, and 10,755%, *PGF2α-R*; 429, 3363, and 6784% at metestrus, diestrus, and proestrus, respectively, compared to estrus) (Fig. 3A and B). In the old CL, expression of these genes was higher at baseline (Fig. 3A and B).

There were differences in mRNA levels between new and old CL. The expression of *SR-BI* mRNA was significantly higher in new CL than in old CL at metestrus. The reverse was observed at estrus and proestrus (Fig. 2A). *StAR* mRNA expression tended to be higher in old CL than in new CL throughout the estrous cycle, and was significantly higher at estrus, diestrus, and proestrus stages (Fig. 2B). *P450scc* and 3β-*HSD* mRNA levels had similar patterns, both of them being significantly higher in new CL than in old CL at metestrus, although there were no differences at the other estrous

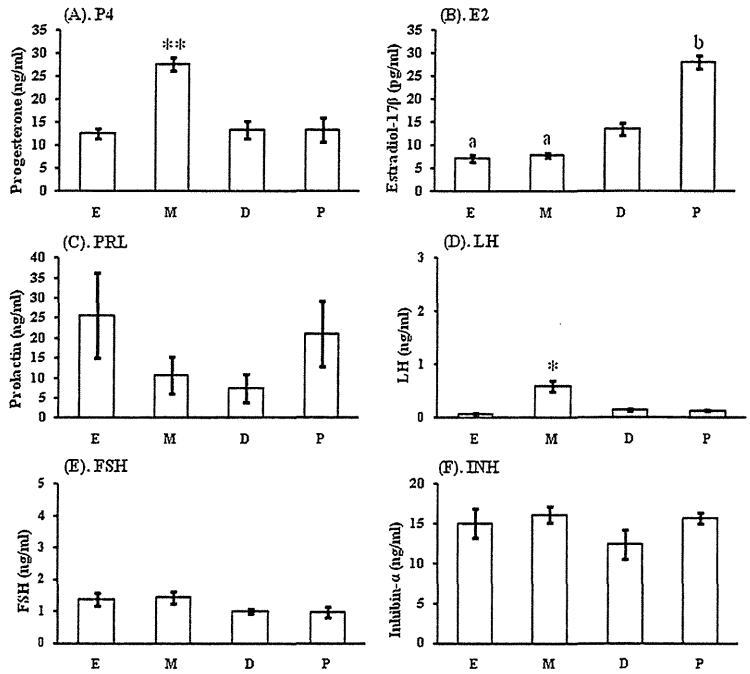

Fig. 1. Serum hormone levels at each estrous cycle stage. Data represent serum P4 (A), E_2 (B), PRL (C), LH (D), FSH (E), and INH (F) levels (mean ± SEM) at each estrous stage (E: estrus; M: metestrus; D: diestrus; P: proestrus). Six to seven animals were examined ($n = 6–7$). Double asterisks ($P < 0.01$), asterisk ($P < 0.05$) and letters ($P < 0.01$) indicate significant differences.

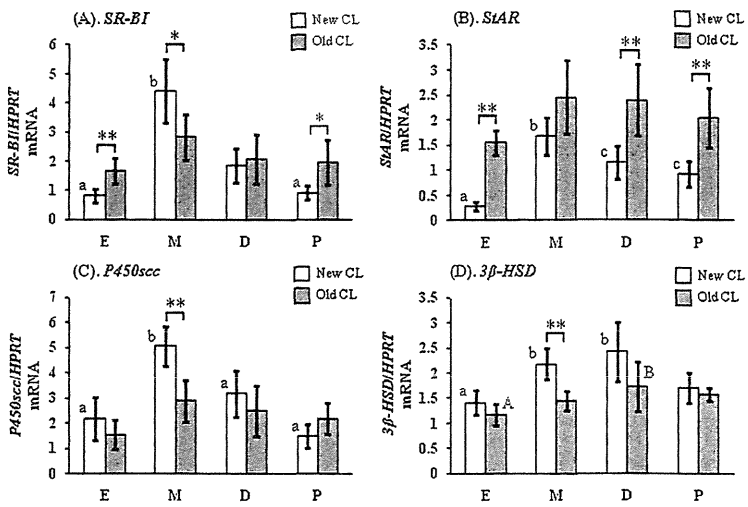

Fig. 2. The mRNA levels of steroidogenic factors in new and old CL across the estrous cycle. Relative mRNA levels of *SR-BI* (A), *StAR* (B), *P450scc* (C), and 3β-*HSD* (D) were presented at each estrous stage (E: estrus; M: metestrus; D: diestrus; P: proestrus). Five animals were examined. Data were normalized for *HPRT* mRNA levels in each sample and presented as the mean ± SD, with asterisks and letters indicating significant differences (**$P < 0.01$; *$P < 0.05$; letters $P < 0.05$).

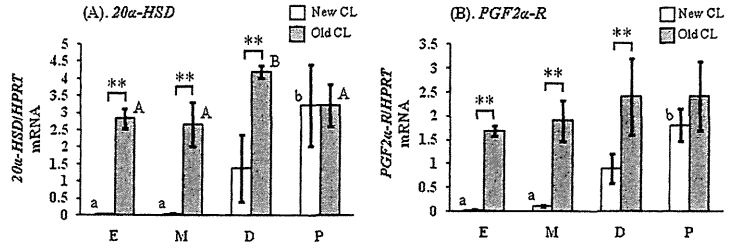

Fig. 3. The mRNA levels of luteolytic factors in new and old CL across the estrous cycle. Relative mRNA levels of 20α-*HSD* (A) and *PGF2α-R* (B) were presented at each estrous stage (E: estrus; M: metestrus; D: diestrus; P: proestrus). Five animals were examined. Data were normalized for *HPRT* mRNA levels in each sample and presented as the mean ± SD, with asterisks and letters indicating significant differences (**$P<0.01$; different letters $P<0.05$).

stages (Fig. 2C and D). 20α-*HSD* and *PGF2α-R* mRNA levels also had similar patterns, but those were much lower in new CL than in old CL at estrus, metestrus, and diestrus stages (Fig. 3A and B). Thus, 20α-*HSD* and *PGF2α-R* mRNA levels were drastically different between new and old CL.

3.3. Immunohistochemical examination of P450scc and 3β-HSD in new and old CL across the estrous cycle

The P450scc- and 3β-HSD-positive luteal cells were observed in all CL throughout the estrous cycle (Figs. 4 and 5). In new CL, the P450scc immunostaining intensity was weak at estrus, but was intensely expressed at the other estrous stages (metestrus, diestrus, and proestrus) (Fig. 4a, c, e, and g). The luteal cells of new CL at metestrus, diestrus, and proestrus stages were strongly and uniformly stained (Fig. 4a, c, e, and g). In contrast, the P450scc-positive luteal cells were observed throughout the estrous cycle in old CL (Fig. 4b, d, f, and h). P450scc strongly positive luteal cells were decreased and scattered in old CL at all stages (Fig. 4b, d, f, and h), and the staining intensities gradually weakened as the CL aged. The profiles of 3β-HSD-positive luteal cells were quite similar to those of P450scc, with the exception of being somewhat weaker (Fig. 5).

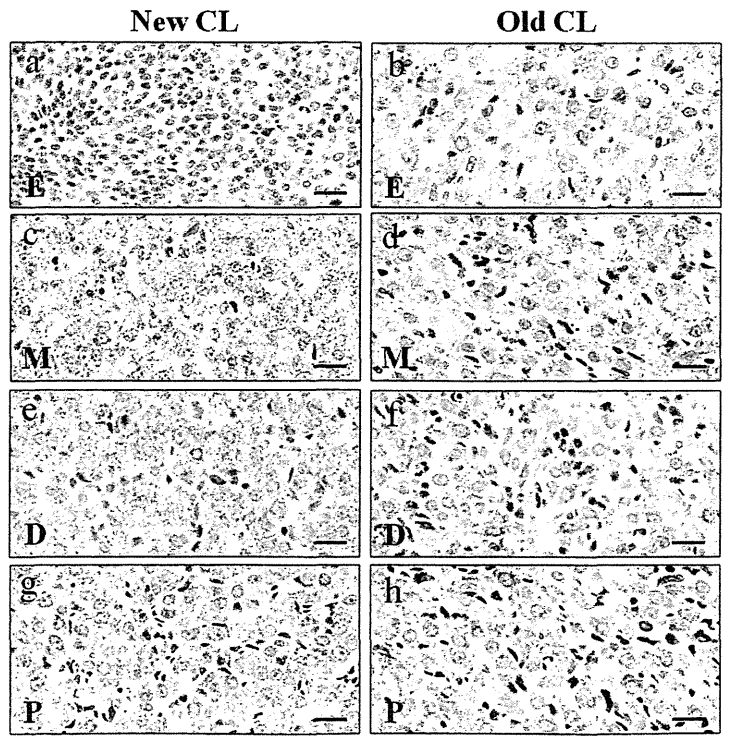

Fig. 4. Immunohistochemistry of P450scc in the cycling rat CL. The left-side pictures (a, c, e, and g) represent new CL, and right-side ones (b, d, f, and h) represent old CL at each estrous stage (E: estrus; M: metestrus; D: diestrus; P: proestrus). Bars indicate 20 μm.

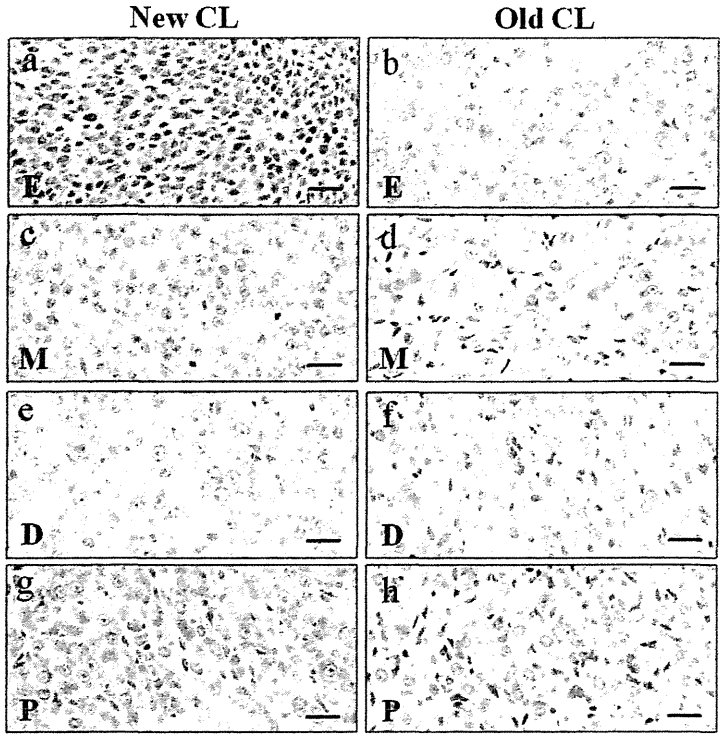

Fig. 5. Immunohistochemistry of 3β-HSD in the cycling rat CL. The left-side pictures (a, c, e, and g) represent new CL, and right-side ones (b, d, f, and h) represent old CL at each estrous stage (E: estrus; M: metestrus; D: diestrus; P: proestrus). Bars indicate 20 μm.

4. Discussion

This study investigated the transition of steroidogenic and luteolytic gene levels in new and old CL in normal cycling rats using the LMD method. Our results demonstrated drastic changes in the gene expression in new CL across the estrous cycle. In the hormone analysis, a significantly higher level of serum P4 in the forenoon at metestrus and the gradual elevation in the E_2 level from estrus to proestrus were consistent with prior reports (Kaneko et al., 1986; Smith et al., 1975; Watanabe et al., 1990). The elevation of LH at metestrus gyrated within the background range. It confirmed that the serum P4 elevation at metestrus was independent of other hormone levels.

In accordance with elevation of serum P4, the steroidogenic genes, *SR-BI*, *StAR*, and *P450scc* mRNA expression peaked at metestrus in new CL then gradually declined. In contrast, those of old CL remained somewhat elevated, making these three steroidogenic genes useful markers for P4 production in new CL. Li et al. (1998) reported that the expression of *SR-BI* mRNA remarkably increased with the completion of luteinization in rats. The reason for this discrepancy remains unclear, but may be explained by differences in experimental conditions. In the previous report, the experimental model employed immature rats treated with equine chronic gonadotropin (eCG) and human chorionic gonadotropin (hCG), whereas mature intact cycling rats were used in the present study.

The present study showed no significant differences in the *P450scc* and 3β-*HSD* mRNA levels between new and old CL except at metestrus. *StAR* mRNA expression in old CL was consistently higher than that in new CL throughout the estrous cycle. This suggests an increased capacity for steroidogenesis in luteal cells of old CL compared to those in new CL. In the present study, the immunohistochemical expression of P450scc did not correspond to mRNA expression. P450scc-positive cells were observed in all CL throughout the estrous cycle. Although the mRNA level was relatively high throughout the estrous cycle, immunohistochemical staining was very slight at estrus in new CL. It is plausible that new CL at estrus may lack the functional maturity required to express P450scc protein. The P450scc staining intensity was gradually weakened as the CL aged. This weak intensity may be attributed to increased interstitial cells in the regressing old CL.

The immunohistochemical expression of 3β-HSD also failed to parallel its mRNA expression. A relatively high level of mRNA was present in all CL throughout the estrous cycle; however, only slight immunoreactivity was present at estrus in new CL. The weak reactions were also considered a reflection of the immaturity of new CL at estrus. The 3β-HSD staining intensity was also gradually weakened as the CL aged, and this again may have been due to the increased interstitial cells in the regressing old CL. Unlike the other steroidogenic factors, the expression of 3β-*HSD* mRNA in new CL was consistently high until diestrus in the present study. In immature rats treated with eCG and hCG, luteal 3β-

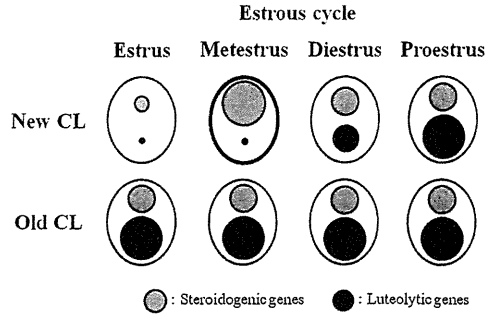

Fig. 6. Overview of steroidogenic and luteolytic gene levels in new and old CL across the estrous cycle in rats. The sizes of the circles represent the levels of steroidogenic genes (gray circles) and luteolytic genes (black circles). The new CL at metestrus, which have the capacity for P4 secretion, showed notably high steroidogenic gene and low luteolytic gene levels. Luteolytic genes in new CL were remarkably low at estrus and metestrus, and gradually increased thereafter. In the old CL, relatively high steroidogenic and markedly high luteolytic gene levels were consistently retained throughout the estrous cycle.

HSD mRNA expression is drastically increased as the CL is formed, with expression sustained throughout the pseudopregnant state (Kaynard et al., 1992). It is suggested that the 3β-HSD expression has a high threshold level of down-regulation by luteolytic factors including PGF2α at diestrus, which is the first stage of functional regression.

The luteolytic genes in new CL showed drastic changes across the estrous cycle ranging from extremely low from estrus to metestrus with a gradual increase thereafter. The transition of 20α-*HSD* mRNA was similar to that of *PGF2α-R*, consistent with 20α-*HSD* mRNA being upregulated by PGF2α. The elevations of 20α-*HSD* and *PGF2α-R* mRNA caused functional luteolysis at diestrus in new CL. The functional luteolysis of new CL starts at diestrus (Sugino and Okuda, 2007). PGF2α plays a crucial role in this process. Administration of PGF2α induces a drop in levels of circulating P4 in rodents (Pharriss and Wyngarden, 1969). In rodents, this reduction of luteal P4 secretion by PGF2α is not the result of decreased synthesis of P4, but rather due to the metabolism of P4 to 20α-DHP (Stocco et al., 2007). PGF2α stimulates the expression of the 20α-*HSD* gene and the activity of this enzyme (Stocco, 2001; Strauss and Stambaugh, 1974) by inducing the expression of the nuclear orphan receptor and transcription factor Nur77, which leads to the transcriptional stimulation of 20α-HSD in the CL (Stocco et al., 2000). The circulating level of 20α-DHP throughout the estrous cycle was previously reported (Nequin et al., 1979), which showed low level during metestrus to diestrus and high level during proestrus to estrus. It seemed that the elevation of 20α-DHP level during proestrus to estrus was attributed to the functionally regressed new CL from diestrus.

An overview of luteal gene expression during the estrous cycle is presented in Fig. 6. The present study found a drastic change in luteal function across the estrous cycle. Our results indicate that both high expression of steroidogenic genes and low expression of luteolytic genes are required for P4 secretion in newly formed CL in a normal estrous cycle. The elevation of luteolytic factors, 20α-HSD and PGF2α-R, plays an important role in the drop of P4 production. Additionally, old CL seemed to have steroidogenic function throughout the estrous cycle, but the P4 produced by them was invariably converted into inactive 20α-DHP by 20α-HSD.

To our knowledge, our study is the first report demonstrating the changes in steroidogenic and luteolytic gene expressions in new and old CL during the estrous cycle with the LMD method. The present study demonstrated that LMD is a useful tool to link the structural and functional changes of each component in the ovary including the CL and follicles. In addition, the results in the present study indicate that consideration of the functional and structural changes in the CL is very important for detecting ovarian toxicants targeting CL, and the changes of steroidogenic and luteolytic gene levels may have a crucial role in onset of lutel toxicity. However, as our study mainly focused on gene expression, additional studies are needed to document these changes on the protein level.

Acknowledgments

We thank Ms. Tomomi Morikawa, Ms. Ayako Kaneko, and Ms. Yoshimi Komatsu for their excellent technical assistance. We also appreciate Dr. Satoru Hosokawa and Dr. Akira Inomata (Drug Safety Japan, Global Drug Safety, Biopharmaceutical Assessments Core Function Unit, Eisai Product Creation Systems, Eisai Co., Ltd.) for their helpful suggestions. This study was supported by Health and Labour Sciences Research Grants, Research on Risk of Chemical Substances, Ministry of Health, Labour and Welfare [H22-Toxicol-003].

References

Acton S, Rigotti A, Landschulz KT, Xu S, Hobbs HH, Krieger M. Identification of scavenger receptor SR-BI as a high density lipoprotein receptor. Science 1996;271:518–20.
Bowen JM, Keyes PL. Repeated exposure to prolactin is required to induce luteal regression in the hypophysectomized rat. Biol Reprod 2000;63:1179–84.
Bruot BC, Wiest WG, Collins DC. Effect of low density and high density lipoproteins on progesterone secretion by dispersed corpora luteal cells from rats treated with aminopyrazolo-(3,4-d)pyrimidine. Endocrinology 1982;110:1572–8.
Dodo T, Taketa Y, Sugiyama M, Inomata A, Sonoda J, Okuda Y, et al. Collaborative work on evaluation of ovarian toxicity. (11) Two- or four-week repeated-dose studies and fertility study of ethylene glycol monomethyl ether in female rats. J Toxicol Sci 2009;34(Suppl. 1):SP121–8.
Gaytan F, Morales C, Bellido C, Aguilar R, Millan Y, Martin De Las Mulas J, et al. Progesterone on an oestrogen background enhances prolactin-induced apoptosis in regressing corpora lutea in the cyclic rat: possible involvement of luteal endothelial cell progesterone receptors. J Endocrinol 2000;165:715–24.
Hamada T, Watanabe G, Kokuho T, Taya K, Sasamoto S, Hasegawa Y, et al. Radioimmunoassay of inhibin in various mammals. J Endocrinol 1989;122:697–704.
Ito A, Mafune N, Kimura T. Collaborative work on evaluation of ovarian toxicity. (4) Two- or four-week repeated dose study of 4-vinylcyclohexene diepoxide in female rats. J Toxicol Sci 2009;34(Suppl. 1):SP53–8.
Kaneko S, Sato N, Sato K, Hashimoto I. Changes in plasma progesterone, estradiol, follicle-stimulating hormone and luteinizing hormone during diestrus and ovulation in rats with 5-day estrous cycles: effect of antibody against progesterone. Biol Reprod 1986;34:488–94.
Kaynard AH, Periman LM, Simard J, Melner MH. Ovarian 3 beta-hydroxysteroid dehydrogenase and sulfated glycoprotein-2 gene expression are differentially regulated by the induction of ovulation, pseudopregnancy, and luteolysis in the immature rat. Endocrinology 1992;130:2192–200.
Li X, Peegel H, Menon KM. In situ hybridization of high density lipoprotein (scavenger, type 1) receptor messenger ribonucleic acid (mRNA) during folliculogenesis and luteinization: evidence for mRNA expression and induction by human chorionic gonadotropin specifically in cell types that use cholesterol for steroidogenesis. Endocrinology 1998;139:3043–9.
Nequin LG, Alvarez J, Schwartz NB. Measurement of serum steroid and gonadotropin levels and uterine and ovarian variables throughout 4 day and 5 day estrous cycles in the rat. Biol Reprod 1979;20:659–70.
Oonk RB, Krasnow JS, Beattie WG, Richards JS. Cyclic AMP-dependent and -independent regulation of cholesterol side chain cleavage cytochrome P-450 (P-450scc) in rat ovarian granulosa cells and corpora lutea. cDNA and deduced amino acid sequence of rat P-450scc. J Biol Chem 1989;264:21934–42.
Peluffo MC, Bussmann L, Stouffer RL, Tesone M. Expression of caspase-2, -3, -8 and -9 proteins and enzyme activity in the corpus luteum of the rat at different stages during the natural estrous cycle. Reproduction 2006;132:465–75.
Peng L, Arensburg J, Orly J, Payne AH. The murine 3beta-hydroxysteroid dehydrogenase (3beta-HSD) gene family: a postulated role for 3beta-HSD VI during early pregnancy. Mol Cell Endocrinol 2002;187:213–21.
Pharriss BB, Wyngarden LJ. The effect of prostaglandin F 2alpha on the progestogen content of ovaries from pseudopregnant rats. Proc Soc Exp Biol Med 1969;130:92–4.
Plas-Roser S, Muller B, Aron C. Estradiol involvement in the luteolytic action of LH during the estrous cycle in the rat. Exp Clin Endocrinol 1988;92:145–53.
Roughton SA, Lareu RR, Bittles AH, Dharmarajan AM. Fas and Fas ligand messenger ribonucleic acid and protein expression in the rat corpus luteum during apoptosis-mediated luteolysis. Biol Reprod 1999;60:797–804.

Sakurada Y, Shirota M, Inoue K, Uchida N, Shirota K. New approach to in situ quantification of ovarian gene expression in rat using a laser microdissection technique: relationship between follicle types and regulation of inhibin-alpha and cytochrome P450 aromatase genes in the rat ovary. Histochem Cell Biol 2006;126:735–41.

Schuler LA, Langenberg KK, Gwynne JT, Strauss 3rd JF. High density lipoprotein utilization by dispersed rat luteal cells. Biochim Biophys Acta 1981;664:583–601.

Slot KA, Voorendt M, de Boer-Brouwer M, van Vugt HH, Teerds KJ. Estrous cycle dependent changes in expression and distribution of Fas, Fas ligand, Bcl-2, Bax, and pro- and active caspase-3 in the rat ovary. J Endocrinol 2006;188:179–92.

Smith MS, Freeman ME, Neill JD. The control of progesterone secretion during the estrous cycle and early pseudopregnancy in the rat: prolactin, gonadotropin and steroid levels associated with rescue of the corpus luteum of pseudopregnancy. Endocrinology 1975;96:219–26.

Stocco C, Callegari E, Gibori G. Opposite effect of prolactin and prostaglandin F(2 alpha) on the expression of luteal genes as revealed by rat cDNA expression array. Endocrinology 2001;142:4158–61.

Stocco C, Telleria C, Gibori G. The molecular control of corpus luteum formation, function, and regression. Endocr Rev 2007;28:117–49.

Stocco CO, Zhong L, Sugimoto Y, Ichikawa A, Lau LF, Gibori G. Prostaglandin F2alpha-induced expression of 20alpha-hydroxysteroid dehydrogenase involves the transcription factor NUR77. J Biol Chem 2000;275:37202–11.

Stocco DM. StAR protein and the regulation of steroid hormone biosynthesis. Annu Rev Physiol 2001;63:193–213.

Strauss 3rd JF, Stambaugh RL. Induction of 20 alpha-hydroxysteroid dehydrogenase in rat corpora lutea of pregnancy by prostaglandin F-2 alpha. Prostaglandins 1974;5:73–85.

Sugino N, Okuda K. Species-related differences in the mechanism of apoptosis during structural luteolysis. J Reprod Dev 2007;53:977–86.

Takahashi M, Iwata N, Hara S, Mukai T, Takayama M, Endo T. Cyclic change in 3 alpha-hydroxysteroid dehydrogenase in rat ovary during the estrous cycle. Biol Reprod 1995;53:1265–70.

Taya K, Mizokawa T, Matsui T, Sasamoto S. Induction of superovulation in prepubertal female rats by anterior pituitary transplants. J Reprod Fertil 1983;69:265–70.

Taya K, Watanabe G, Sasamoto S. Radioimmunoassay for progesterone, testosterone, and estradiol-17β using 125I-iodohistamine radioligands. Jpn J Anim Reprod 1985;31:186–97.

Tebar M, Ruiz A, Gaytan F, Sanchez-Criado JE. Follicular and luteal progesterone play different roles synchronizing pituitary and ovarian events in the 4-day cyclic rat. Biol Reprod 1995;53:1183–9.

Watanabe G, Taya K, Sasamoto S. Dynamics of ovarian inhibin secretion during the oestrous cycle of the rat. J Endocrinol 1990;126:151–7.

Yadav VK, Lakshmi G, Medhamurthy R. Prostaglandin F2alpha-mediated activation of apoptotic signaling cascades in the corpus luteum during apoptosis: involvement of caspase-activated DNase. J Biol Chem 2005;280:10357–67.

Yoshida M, Sanbuissyo A, Hisada S, Takahashi M, Ohno Y, Nishikawa A. Morphological characterization of the ovary under normal cycling in rats and its viewpoints of ovarian toxicity detection. J Toxicol Sci 2009;34(Suppl. 1):SP189–97.

Yuan Y, Foley G. Female reproductive system. In: Haschek WM, Rousseaux CG, Wallig MS, editors. Handbook of toxicologic pathology. 2nd ed. London: Academic Press; 2002. p. 847–94.

Cancer Science
The official journal of the Japanese Cancer Association JCA

Development of an early induction model of medulloblastoma in Ptch1 heterozygous mice initiated with *N*-ethyl-*N*-nitrosourea

Miwa Takahashi,[1,4] Saori Matsuo,[1,2] Kaoru Inoue,[1] Kei Tamura,[1] Kaoru Irie,[1] Yukio Kodama[3] and Midori Yoshida[1]

[1]Division of Pathology, National Institute of Health Sciences, Setagaya-ku, Tokyo; [2]Pathogenetic Veterinary Science, United Graduate School of Veterinary Sciences, Gifu University, Gifu; [3]Division of Toxicology, National Institute of Health Sciences, Setagaya-ku, Tokyo, Japan

(Received June 1, 2012/Revised August 1, 2012/Accepted August 22, 2012/Accepted manuscript online August 31, 2012/Article first published online October 30, 2012)

Mice heterozygous for the *ptch1* gene (ptch1 mice) are known as a valuable model of medulloblastoma, a common brain tumor in children. To increase the incidence and reduce the time required for tumor development, allowing for evaluation of modifier effects on medulloblastoma in a short time, we attempted to develop an early induction model of medulloblastoma in ptch1 mice initiated with *N*-ethyl-*N*-nitrosourea (ENU). Ptch1 mice and their wild-type littermates received a single intraperitoneal injection of ENU (10, 50 or 100 mg/kg) on postnatal day 1 (d1) or 4 (d4), and histopathological assessment of brains was conducted at 12 weeks of age. The width of the external granular layer (EGL), a possible origin of medulloblastoma, after injection of 100 mg ENU on d1 or d4 was measured in up to 21-day-old mice. Cerebellar size was apparently reduced at the 50 mg dose and higher regardless of genotype. Microscopically, early lesions of medulloblastomas occurred with a high incidence only in ptch1 mice receiving 10 mg on d1 or d4, but a significant increase was not observed in other groups. Persistent EGL cells and misalignment of Purkinje cells were increased dose-dependently. Although EGL was strikingly decreased after ENU injection, strong recovery was observed in mice of the d1-treated group. In summary, neonatal treatment with ENU is available for the induction of medulloblastoma in ptch1 mice, and 10 mg of ENU administered on d1 appeared to be an appropriate dose to induce medulloblastoma. (*Cancer Sci* 2012; 103: 2051–2055)

Medulloblastoma, a primitive neuroectodermal tumor that develops in the cerebellum, is the most common brain tumor of childhood.[1] The etiology of childhood brain tumors remains largely unknown, but previous studies have suggested associations between childhood brain tumors and chemicals such as pesticides and nitrates.[2–4] These studies are mainly epidemiological, and there are few investigations into the effects of chemical exposure during development on childhood tumor using animal models.

Recent genomic approaches have demonstrated the existence of four distinct subtypes with demographic, transcriptional profiles and clinical outcome.[5,6] In these subtypes, the tumors with activation of the Sonic hedgehog (Shh)-Ptch signaling pathway belong to the SHH group, and are considered to arise from granule cell precursors (GCPs) in the external granular layer (EGL) of the developing cerebellum.[7] Since Shh signaling is known to drive proliferation in the GCPs, it has been suggested that the pathway dysregulation resulting from genomic alterations of its components presumably drives medulloblastoma formation.[7]

Mice heterozygous for the *ptch1* gene (ptch1 mice) are an important model for medulloblastoma. Homozygous knockout mice die during embryonic development with defects in the nervous system.[8] Heterozygous mice survive to adulthood, and 14–20% develop medulloblastoma several months after birth.[8,9] Histological and marker expression analysis of the brain tumor has revealed that they closely resemble human medulloblastoma,[9] and similar to human cases, the origin of medulloblastoma in ptch1 mice is thought to be residual EGL cells that failed to exit proliferation.[10] Activation of the Shh pathway has also been confirmed in the tumors of ptch1 mice,[9] and this mouse model is equivalent to the SHH group in human cases. While the study of the molecular mechanism underlying medulloblastoma formation has progressed, few studies on the modifying effects of chemicals on tumor development have been conducted.

Although ptch1 mice are a valuable model for studying medulloblastoma, the low frequency and long latency for tumor development are disadvantages for detection of the modulatory effects on medulloblastomas, especially in the case of tumor suppressive compounds. Previous reports showed that neonatal irradiation dramatically increased the incidence of medulloblastoma, and it has been suggested that tumorigenesis in ptch1 mice follows a multi-step process.[10–12] So far, medium-term carcinogenicity bioassays based on the multi-step cancer development (initiation promotion model) have been established in many organs to detect modifying effects on tumor development in a short term.[13,14] *N*-ethyl-*N*-nitrosourea (ENU) is a very common initiator and is known to induce nervous system tumors including medulloblastoma in newborn mice.[15,16] Therefore, to increase the incidence and decrease the time required for tumor development, we attempted to induce medulloblastoma using ENU in ptch1 mice.

Materials and Methods

Mice. Ptch1 heterozygous knockout mice, generated by replacing exon 1 and 2 of the *ptch1* gene with a LacZ/neomycin cassette,[8] were obtained from The Jackson Laboratory (Bar Harbor, ME, USA) and maintained in our laboratory. They were housed in polycarbonate cages with wood chip bedding and kept in an air-conditioned animal room with basal diet (CRF-1; Oriental Yeast, Tokyo, Japan) and tap water available *ad libitum*.

Experimental design. Twenty-five dams were used in experiment 1. Ptch1 mice and their wild-type (WT) littermates received a single intraperitoneal injection of ENU (Nacalai Tesque, Kyoto, Japan) dissolved in saline. The highest dose selected was 100 mg/kg based on a previous study,[15,16] and 50 and 10 mg/kg were set as medium and low doses, respectively. Postnatal day 1 (d1) or 4 (d4) was chosen as administration day because they are periods of active proliferation in

[4]To whom correspondence should be addressed.
E-mail: mtakahashi@nihs.go.jp

doi: 10.1111/cas.12006

Table 1. The number and survival rate (%) of ptch1 and wild-type mice examined at 12 weeks of age

Administration day	ENU (mg/kg)	No. of litters	Ptch1 No. (%)	Wild-type No. (%)
–	0 (Control)	5	16 (93.8)	11 (90.9)
d1	10	3	15 (100)	5 (100)
	50	3	15 (93.3)	8 (100)
	100	5	23 (87.0)	5 (100)
d4	10	3	10 (100)	9 (100)
	50	3	10 (90.0)	11 (100)
	100	3	14 (85.7)	6 (83.3)

d1, postnatal day 1; d4, postnatal day 4; ENU, *N*-ethyl-*N*-nitrosourea.

the EGL. Intact mice were used as the controls. Each group was composed of at least 10 ptch1 mice and five WT mice from three to five dams (Table 1). Daily observation for clinical signs and mortality was conducted throughout the study. We set the duration as 12 weeks, because mortality caused by malignant lymphoma increased after 13 weeks of age in a preliminary study. At 12 weeks of age, all animals were subjected to autopsy under deep isoflurane anesthesia. The brains, thymus, spleen and macroscopic lesions were removed and fixed in neutrally-buffered 10% formalin. The tissues were routinely processed for paraffin embedding, sectioned and stained with hematoxylin and eosin.

In experiment 2, ptch1 and WT mice from 16 dams received 100 mg/kg of ENU intraperitoneally on d1 or d4, and the brains of each of the 9–13 mice were removed on d4, 7, 14 or 21. For comparison, the brains from 12 intact mice including both genotypes were also collected at the same time point, respectively, and the tissues were processed routinely for histological examination.

The animal protocol was reviewed and approved by the Animal Care and Use Committee of the National Institute of Health Sciences, Japan.

Histopathology. All cerebella were examined in midsagittal section. Based on a previous report,[17] the stage of neoplastic lesions in the cerebellum was classified according to the size as follows: hyperproliferation of EGL, micronodule, nodule, microtumor and full-blown tumor (Fig. 1).

Persistent EGL cells were classified into the focal lesion and the diffuse or zonal lesions, according to type of distribution. The degrees of focal lesions were divided as follows: grade 1, only one to two very small clusters consisting of about 10 cells; grade 2, a few clusters consisting of about 10–30 cells; and grade 3, several clusters consisting of 30 cells or more in the midsagittal section of the cerebellum. Diffuse lesions were divided as follows: grade 1, persistent EGL cells distributed diffusely in a part of the cerebellum; and grade 2, persistent EGL cells distributed diffusely in most areas of the cerebellum. In addition, when the cell clusters were observed parallel to the granular layer, we classified the lesions into zonal type.

Morphometric assessment. Photomicrographs of midsagittal sections of the cerebellum were taken with a digital camera attached to a microscope (DP71; Olympus, Tokyo, Japan), and measurement was performed using image analysis software (WinROOF, Version 5.7.1; Mitani, Tokyo, Japan). The areas of the cerebellum and granular layer were measured for each genotype, and the animals with a large tumor were eliminated. The average width of the EGL of each mouse was determined by tenth measurements selected at random from the entire cerebellum. Because the width did not differ according to genotype, we counted the values of both mice together.

Statistical analysis. As for data of the areas of the cerebellum and granular layer, values of the d1-treated and d4-treated groups were compared with the corresponding controls by one-way ANOVA or the Kruskal–Wallis test. When statistically significant differences were detected, Dunnett's multiple comparisons test was used for comparison between the control and treatment groups. Incidence of histopathological findings was compared using Fisher's exact probability test. Width of EGL was analyzed by the Student's or Welch's *t*-test following a test for equal variance.

Results

Most mice were asymptomatic throughout the study. Eight ptch1 mice and two WT mice were found dead or moribund. Hydrocephalus was found in three ptch1 mice, and the cause of death in the other cases could not be determined. At 12 weeks of age, there were no intergroup differences in survival rate in both groups (Table 1). A significant difference was not detected in final body weight (data not shown).

Reduction of cerebellar size was apparent at 50 mg regardless of genotype (Fig. 2), and morphometric analysis revealed a significant decrease in the areas of the cerebellum and granular layer in the groups treated with 50 or 100 mg of ENU (Fig. 3).

The incidence of medulloblastoma in ptch1 mice of the control group was 19% (3/16) (Fig. 4). In contrast, 11 of 15 (73%) and six of 10 (60%) mice developed medulloblastoma in the groups receiving 10 mg on d1 or d4, respectively. At 50 mg, medulloblastoma occurred in seven of 15 (47%) mice treated on d1 and in two of 10 (20%) mice treated on d4. At 100 mg, the tumor incidence was 27% (6/22) in d1-treated mice and 29% (4/14) in d4-treated mice. Most were regarded as an early stage of medulloblastoma, and a significant increase in the incidence was detected only in the groups receiving 10 mg. In WT mice, there was no medulloblastoma occurrence in either group.

As previously reported, focal lesions of persistent EGL in subpial position were common in ptch1 mice and occasionally found in WT mice (Fig. 5A). The incidence and degree of subpial EGL foci were not greatly influenced by ENU treatment (Fig. 5E). In contrast, the persistent EGL cells were distributed diffusely in the molecular layer in mice receiving ENU at 10 and 50 mg (Fig. 5B), and the persistent EGL cells showed a

Fig. 1. Neoplastic lesions in the cerebellum. Neoplastic lesions in the cerebellum were classified according to size as follows; (I) hyperproliferation of external granular layer, (II) micronodule, (III) nodule, (IV) microtumor and (V) full-blown tumor. Hematoxylin and eosin section. Bar, 100 μm.

doi: 10.1111/cas.12006